Sergio Tusso[1,2,*], Bart P.S. Nieuwenhuis[1], Bernadette Weissensteiner[1], Simone Immler[2,3], and Jochen B.W. Wolf[1,2,*]

[1] Division of Evolutionary Biology, Faculty of Biology, LMU Munich, Planegg-Martinsried, Germany

[2] Science for Life Laboratories and Department of Evolutionary Biology, Uppsala University, Uppsala, Sweden

[3] School of Biological Sciences, University of East Anglia, Norwich Research Park, Norwich, NR4 7TJ, UK

* Corresponding authors: S. Tusso: email: situssog@gmail.com

J. B.W. Wolf: email: j.wolf@bio.lmu.de

These authors contributed equally: S. Tusso, B. Nieuwenhuis

These authors jointly supervised this work: S. Immler, J. Wolf

Adaptive divergence is the key evolutionary process generating biodiversity by means of natural selection. Yet, the conditions under which it can arise in the presence of gene flow remain contentious. To address this question, we subjected 132 sexually reproducing fission yeast populations sourced from two independent genetic backgrounds to disruptive ecological selection and manipulated the level of migration between environments. Contrary to theoretical expectations, adaptive divergence was most pronounced when migration was either absent ('allopatry') or maximal ('sympatry'), but was much reduced at intermediate rates ('parapatry', 'local mating'). This effect was apparent across central life history components (survival, asexual growth, and mating), but differed in magnitude between ancestral genetic backgrounds. The evolution of some fitness components was constrained by pervasive negative correlations (trade-off between asexual growth and mating), while others changed direction under the influence of migration (e.g. survival and mating). In allopatry, adaptive divergence was mainly conferred by standing genetic variation and resulted in ecological specialization. In sympatry, divergence was mainly mediated by novel mutations enriched in a subset of genes and was characterized by the repeated emergence of two strategies: an ecological generalist and an asexual growth specialist. Multiple loci showed consistent evidence for antagonistic pleiotropy across migration treatments and provide a conceptual link between adaptation and divergence. This evolve-and-resequence experiment demonstrates that rapid ecological differentiation can arise even under high rates of gene flow. It further highlights that adaptive trajectories are governed by complex interactions of gene flow, ancestral variation and genetic correlations.

Main

Adaptive divergence describes the emergence of new forms from a shared common ancestor by adaptation to different environmental conditions. As such, it is key to the formation of new species by means of natural selection [1,2]. In geographic isolation, divergent selection readily promotes ecological specialisation which over time can result in reproductive barriers between populations [3–6]. In the presence of gene flow, however, the conditions enabling adaptive divergence are difficult to predict [7–9]. Homogenizing gene flow may impede adaptive divergence and promote generalist phenotypes exploiting a broader ecological spectrum [10,11]. Alternatively, gene flow may promote divergence by supplying adaptive genetic variation or by modifying genetic correlations which can alter evolutionary constraints and open new evolutionary trajectories [12,13]. In general, the relationship between gene flow and adaptive divergence is expected to decline monotonically (i.e. less divergence with higher gene flow)

60 [14]. Depending on the degree of gene flow, the strength of selection, and the genetic
61 architecture of adaptive traits evolutionary outcomes are ,however, hard to predict: divergence
62 may be precluded, stalled at an intermediate level or progress towards the origin of new
63 species [15–17,14]. Adaptive divergence thus constitutes a necessary, but not sufficient component
64 for ecological speciation. Understanding the conditions under which it arises is of central
65 importance to our understanding of how populations can exploit divergent ecological niches
66 and differentiate into distinct ecotypes that may – or may not – seed novel species [18,19].

67 Genome-wide characterization of genetic variation has spurred progress in the study of
68 ecological divergence with gene flow in the wild [20–22]. However, the idiosyncratic nature and
69 complex evolutionary histories of natural populations impair inference of causal relationships
70 and make it difficult to pinpoint the mechanisms promoting or impeding divergence [8].
71 Controlled experiments elucidating the genetic basis of adaptive divergence and evaluating
72 the role of gene flow are thus needed [23,20,24]. Replicated experimental manipulation of
73 migration between controlled ecological contrasts in evolving populations are a promising,
74 although hitherto largely unexplored way forward [23].

75 Here, we present the results from a long-term experimental evolution study addressing this
76 question in the haploid fission yeast *Schizosaccharomyces pombe*, in which we tested the
77 effect of gene flow and standing variation on genetic and phenotypic adaptation to disruptive
78 selection. A total of 132 populations were maintained for 53 complete reproductive cycles
79 each encompassing ~13 asexual cell divisions. Each cycle comprised asexual growth,
80 followed by ecologically disruptive selection and subsequent sexual reproduction (**Figure**
81 **1a**). Sets of 22 populations were distributed among four treatment groups varying in the
82 amount of migration after disruptive selection (ranging from complete isolation to full
83 mixing; hereafter referred to as 'allopatry', 'parapatry', 'local mating', and 'sympatry',
84 **Figure 1b & Supplementary Figure 1**). As an ecological parameter we used disruptive

viability selection on settling speed by collecting cells from the bottom (bottom selection - B) or the top (top selection - T) in a liquid column after a predefined period of time. Population sizes were in the order of ~$3 \cdot 10^7$ individuals precluding a dominant role of genetic drift. All experimental populations were derived from two ancestral populations (referred as 'α' and 'β') that had experienced the same selection regime in the past but differed in standing genetic variation (see **Methods**). For ease of presentation, we will focus on the results for the α genetic background which in general showed a stronger response to selection. We refer to the β background where it deviates from the α. After 53 cycles of sexual reproduction, we measured fitness relative to the respective ancestral population for four fitness components reflecting major life history traits: asexual growth rate (g), reproductive success (r) and survival during top or bottom selection (top: W_T; or bottom: W_B).

This experiment tests the role of strong divergent ecological selection at four levels of migration. Despite the apparent simplicity of the setup, the experimental life cycle involves a variety of fitness components each of which can be subject to selection, and hence can evolve (e.g. alternation between liquid and solid media, asexual growth, sexual reproduction, survival during ecological selection). Interdependence between fitness components is expected to elicit a correlated response which can promote or constrain adaptive divergence [25,12]. For instance, increased performance during (asexual) growth can result in reduced output during sexual reproduction [26–29]. In addition, ecological adaptation may not result even if a given trait value increases survival, but has negative consequences on a correlated life history trait. Importantly, these correlations need not be static as evolution of one life history trait may alter the strength and direction of selection on another (e.g. differences in asexual growth rate bears on population density and thus nutrient availability). Genetically encoded variance-covariance relationships between life history traits (as represented by the G-matrix [30,31]), and the ability of these relationships to evolve in themselves constitutes an essential component

110 determining the evolutionary trajectory of each population [13]. We anticipate that the influence
111 and stability of these correlations may be contingent on the level of gene flow and play a
112 central role in constraining or facilitating divergence [12].

113 We report the results of this experiment as follows. We first consider the influence of
114 migration and standing genetic variation on adaptive divergence of each fitness component in
115 isolation. In brief, we found that the degree of adaptive divergence overall depended on
116 standing genetic variation, and was strongest at the extreme ends of the gene flow gradient
117 (allopatry and sympatry). We then expand on these results considering the intrinsic
118 correlations between fitness components (G-matrix) which evolved relative to the ancestral
119 populations in response to gene flow and played a central role in facilitating adaptive
120 divergence. Finally, we assess the genetic architecture of divergence by means of whole
121 genome sequencing data for all ancestral and evolved populations (Pool-Seq). Standing
122 genetic variation with evidence for antagonistic pleiotropy was the main driver for ecological
123 specialization in the absence of gene flow. In contrast, divergence in sympatry was
124 characterized by population-specific independent mutations.

125 Results and discussion

126 Migration affects adaptive divergence

127 After 53 cycles of disruptive ecological selection populations showed evidence for evolution
128 across different fitness components (relative fitness difference from ancestral value of 1, see
129 **Figure 2a**). In line with theoretical predictions that isolated populations will readily respond
130 to directional selection[11], allopatric populations of the α background showed evidence for
131 adaptive divergence in three of the four fitness components (g, r and W_T) resulting in
132 specialized top and bottom ecotypes (**Figure 2a, Supplementary Table 1 & 2**). Populations
133 that had exclusively been selected for the top environment (shown in blue across figures)

134 grew faster and survived significantly better during further ecological top selection than
135 populations that had only experienced the bottom environment (shown in red). However, their
136 sexual reproductive success was reduced in comparison to bottom populations. These
137 differences were consistent between populations demonstrating that the disruptive ecological
138 selection regime predictably induced the evolution of specialized strategies for the top and
139 bottom environment (for statistical model see **Supplementary Tables 1 & 2).** Similar
140 divergence across fitness components was observed for the β background, although they
141 showed an overall weaker response and evolved differences in survival after bottom selection
142 rather than for asexual growth. This difference may be related to a diminishing-return
143 relationship for the already higher growth rate of the β ancestor reducing the potential for
144 adaptation in this trait [32] (**Supplementary Fig. 2**).

145 Populations that experienced intermediate levels of migration ('parapatry' and 'local mating')
146 showed a different response. Even though these populations showed changes relative to the
147 ancestor, no divergence between selection regimes was observed for any of the four fitness
148 components (**Figure 2a**). Moreover, in these two treatments, fitness values for the populations
149 evolving as pairs were strongly correlated and highly similar (**Extended Data Fig. 1,**
150 **Supplementary Table 1 & 2**). These results support the prediction that intermediate levels of
151 gene flow tend to homogenize population pairs and constrain divergence [10,33,9].

152 In contrast to expectations that higher migration reduces diversification, sympatric
153 populations, which experienced the highest level of migration, showed evidence for
154 divergence when separating each population into two fractions (top and bottom) followed by
155 two continued cycles of disruptive selection without gene flow (see **methods and discussion**
156 **below**). Similar to divergence between populations under allopatry (i.e. no gene flow),
157 divergence was evident between sympatric top and bottom fractions for three of the fitness
158 components (g, W_T, W_B). In contrast to allopatry and expected for a high gene flow regime[34],

159 the bottom fraction had evolved a generalist survival strategy outperforming the top fraction
160 in both the top and bottom environment **(Figure 2a**). Importantly, however, the top selected
161 fraction showed increased fitness only during asexual growth, suggesting the emergence of a
162 polymorphism between an ecological generalist and a growth specialist (see below). The local
163 mating treatment expected to foster divergence [35,36] did not result in similar ecotypic sub-
164 functionalisation. Results from the β background were comparable, showing most divergence
165 in allopatry and sympatry, followed by parapatry and least in the local mating treatment
166 (**Figure 2a & Extended Data Fig. 1**). In summary, adaptive divergence evolved more readily
167 in the α genetic background and was most pronounced at the extreme end of the migration
168 gradient. In allopatry, it resulted in the emergence of top and bottom specialists, whereas in
169 sympatry we observed a polymorphism between an ecological generalist and a growth
170 specialist.

171

172 Genetic correlations and G-matrix evolution

173 Consistent with expectations [25,12], evolutionary responses of the various fitness components
174 were governed by intrinsic correlations. To investigate the direction, strength and
175 evolutionary stability of these correlations, we constructed standardized variance-covariance
176 matrices (G-matrices) for all four fitness components: asexual growth rate (g), reproductive
177 success (r) and survival to top (W_T) or bottom selection (W_B) (**Figure 2b**). Positive parameter
178 values for a given pair of components indicate consistent evolutionary responses across all
179 evolved populations for both fitness components. Negative parameter values indicate an
180 increase in one component accompanied by a decrease in the other component, suggesting a
181 classical trade-off. We observed a pervasive negative relationship between growth rate and
182 sexual reproductive success across all migration treatments and genetic backgrounds (**Figure**

183 **2b**) despite large differences in growth rate between ancestral populations (**Supplementary**
184 **Figure 2)**. Other relationships, such as a negative correlation between survival during top
185 selection and growth, or a positive correlation between survival during bottom selection and
186 sexual reproduction were dependent on the amount of migration (**Figure 2b**). Additionally,
187 correlations between fitness components were contingent on the genetic background.
188 Correlations were more consistent for different migration treatments in the β background
189 possibly due to the lower degree of adaptive divergence observed for these populations.
190 Analysing the covariance in fitness components using Principal Component Analysis with
191 normalized fitness values confirmed these findings (**Extended Data Fig. 2**). In summary,
192 phenotypic evolution was strongly governed by intrinsic correlation and potential trade-offs,
193 but correlations between fitness components varied in their stability and were influenced by
194 the level of gene flow and genetic background.

195

196 ## Genetic correlations and adaptive divergence

197 Above, we have shown that adaptive divergence was most pronounced in allopatry and
198 sympatry, particularly in the α genetic background. In allopatry, directional ecological
199 selection in a given environment elicited a correlated response in sexual reproduction (α & β
200 background) and growth (α background). The direction of the response defined top or bottom
201 specialists (top: high fitness for growth, low for sexual reproduction; bottom: low for growth,
202 high for sexual reproduction; **Figure 2a**). In contrast, populations exposed to maximal levels
203 of migration (sympatry) experienced both top and bottom selection environments during each
204 cycle and developed a generalist ecological strategy. This generalist strategy showed high
205 performance in both environments as well as in sexual reproduction (**Figure 2a**). However,
206 due to the pervasive trade-off of these components with asexual growth (**Figure 2b**),
207 populations could not increase fitness for all life-history components simultaneously. In

208 populations of the α background, this trade-off was consistently resolved by an intra-
209 population polymorphism: a bottom generalist performing well in both environments and
210 sexual reproduction, and a top specialist with high performance for speed during asexual
211 growth (**Figure 2a**). Overall, these analyses highlight the importance of gene flow on the
212 evolution of genetic correlations and their impact on adaptive divergence.

213

214 Migration and the partitioning of genetic variation

215 To investigate the genetic basis of adaptive evolutionary change, we inferred population allele
216 frequencies for all 132 evolved populations. At the beginning of the experiment, we identified
217 107 and 114 genetic variants (SNPs and small indels) representing standing genetic variation
218 in the α and β ancestral genetic background, respectively (**Extended Data Fig. 3a**). After 53
219 sexual generations, we counted a total of 1,472 (α background) and 1,318 variants (β
220 background) ranging from 71 to 183 variants per population. Most variants were present at
221 low frequencies (~80% with maximum frequency < 0.2), and/or limited to single populations
222 (~62% of all variants) (**Extended Data Fig. 3b**).

223

224 To test for genetic differentiation between top and bottom environments, we first performed
225 Principal Component Analyses (PCA) using allele frequencies of allopatric populations. We
226 observed that genetic variation of allopatric populations was partitioned according to selection
227 regime. Top and bottom populations diverged from the ancestor in opposite directions along
228 the main axis of variation (**Figure 3a, Extended Data Fig. 4;** linear model on PCA1 by
229 ecological selection regime, $p<1.0 \times 10^{-3}$ for both genetic backgrounds). The clustering by
230 selection regime is best explained by parallel allele frequency shifts of standing genetic
231 variation due to ecological selection. Separation of populations into top and bottom clusters
232 thus provides evidence for allelic separation of shared, ancestral genetic variants by top and

233 bottom ecotypes (further discussed in 'Genetic architecture of genetic variation'). Consistent
234 with this interpretation measures of genetic divergence, D_{xy} and F_{st}, were highest between top
235 and bottom ecotypes only when considering standing genetic variation (**Extended Data Fig.**
236 **5 & 6)**.

237 In contrast, parapatric populations showed no consistent genetic differentiation between
238 connected top and bottom population pairs neither for standing variation nor genome-wide
239 (**Extended Data Fig. 5 & 6).** Instead, pairs of parapatric populations were genetically more
240 similar to each other than to populations from the same selection regime suggesting
241 homogenization by gene flow. Yet, while gene flow inhibited genetic divergence, it did not
242 exclude evolution per se. Genetic variation across independent population pairs was
243 comparable to the genotypic space (PC1 and PC2) of allopatric top and bottom specialists
244 (**Figure 3a**, **Extended Data Fig. 5 & 6**). Local mating populations also spanned a broad
245 range of genetic variation, though clustered primarily with allopatric bottom populations
246 (**Figure 3a**). Populations evolving in sympatry exclusively carried a signature of genetic
247 variation characteristic for allopatric bottom populations (**Figure 3a,** Sym_Allo_B vs.
248 Sym_Allo_T in **Extended Data Fig. 5 & 6**).

249 These findings suggest that a moderate amount of gene flow (parapatry) still allows
250 populations to accumulate genetic variation that is beneficial to both ends of the disruptive
251 selection regime, but precludes adaptive divergence between connected population pairs.
252 With increasing levels of gene flow, however, one ecological condition (here bottom selection
253 regime) appears to dominate the component of standing genetic variation responding to
254 selection. While this pattern is consistent with the observed increase in fitness for bottom
255 selection in the sympatric bottom ecotype, it fails to explain the simultaneous increase for
256 fitness components responding to top selection (sympatry) or the shift in the G-matrix (local
257 mating, sympatry). In sympatry, where phenotypic data suggest coexistence of an ecological

258 generalist bottom ecotype and a growth specialist (**Figure 2a)** this implies an additional role
259 of population-specific novel mutations allowing divergence of these strategies.

260 In order to test for genetic divergence between ecotypes, we additionally sequenced
261 subpopulations after two rounds of top and bottom selection from sympatric and local mating
262 populations. In the α background, net sequence divergence (D_a, [37]) was positive for all
263 populations indicating genetic differentiation between top and bottom ecotypes. Genetic
264 divergence was higher in sympatry compared to local mating mirroring patterns of phenotypic
265 divergence (**Extended Data Fig. 7**). Sympatric divergence was further characterized by
266 genetic variants increasing in frequency during both top and bottom selection, with a
267 significant skew towards top selected variants which was not observed in local mating
268 populations (**Extended Data Fig. 8**). Moreover, selection-induced changes in allele
269 frequencies were less pronounced after top selection suggesting that the pool population may
270 be dominated by variants beneficial to the top ecotype (**Extended Data Fig. 8**). Assuming no
271 systematic bias in effect sizes between variants, these results are consistent with the idea of
272 co-existing strategies in α sympatric populations rather than exclusive dominance of a bottom
273 generalist ecotype. In contrast, for sympatric ecotypes of the β background, net divergence
274 was similarly low as for local mating populations, and allele frequency shifts showed no
275 major contribution of top selected variants (**Extended Data Fig. 7 & 8**). In conjunction with
276 the phenotypic data, these results may indicate that these populations are mainly dominated
277 by a bottom generalist ecotype lacking evidence for polymorphism with a growth specialist
278 (**Figure 2a)**. Interestingly, these data suggest that local mating also contains genetically
279 differentiated subpopulations despite clear divergence for the life history traits we measured.
280 In summary, the genetic data suggests different modes of adaptation depending on the degree
281 of gene flow. In allopatry, ecological specialization resulted from parallel allele frequency

282 shifts of standing genetic variation, whereas in sympatry (α background) independent, novel
283 mutations appear to repeatedly induce a polymorphism of strategies.

284

285 Genetic architecture of adaptive variation

286 As expected from the large experimental population sizes, the genetic composition of evolved
287 populations was found to be governed by ecological selection, and not genetic drift. In
288 allopatric populations, the importance of selection for driving the correlation between traits
289 was illustrated by the fact that the major axes of genetic variation (**Figure 3a**) and variation in
290 fitness components (**Extended Data Fig. 2**) were strongly correlated (**Figure 3b**, PC1:
291 $R_{adj.}^2 = 0.69$, $p < 0.0001$, PC2: $R_{adj.}^2 = 0.16$, $p = 0.021$). In the presence of gene flow
292 (parapatry), the correlation was reduced and only significant for the main axis of variation
293 (PC1: $R_{adj.}^2 = 0.15$, $p = 0.037$; PC2: $R_{adj.}^2 = 0.04$, $p = 0.31$). In β populations, where the
294 divergence between allopatric top and bottom populations was weaker, the correlation was
295 not statistically supported (PC1: $p = 0.1$, $R_{adj.}^2 = 0.07$; PC2: $p = 0.7$, $R_{adj.}^2 = 0.04$). Individual
296 based simulations mirroring the allopatric experimental setup further supported that the
297 observed increase in allele frequency of novel mutations was the result of ecological selection
298 rather than drift (**Supplementary Figures 5 & 6**). Moreover, mutations with low predicted
299 functional effects (synonymous sites, non-coding regions) segregated at low frequencies,
300 whereas mutations with moderate (missense variant, codon loss/gain) and strong predicted
301 effects (frame shift, stop gain, start loss) increased to significantly higher frequencies in all
302 populations (**Extended Data Fig. 9**). This disproportionately strong increase in frequency of
303 mutations with strong predicted effects was pervasive across all levels of migration
304 (**Supplementary Figure 7**).

305 Next, we quantified the degree of parallelism in allele frequency shifts. 34 and 50 genetic
306 variants corresponding to 32 % and 44% of all standing genetic variation from the α and β
307 background, respectively, showed consistent differences in the direction of allele frequency
308 changes between allopatric top and bottom populations (**Extended Data Fig. 10**). However,
309 only five (α) and three (β) genetic variants reached frequencies above 0.9 for at least two
310 populations in one ecological regime while going extinct in the opposite regime for most
311 populations. These same variants contributed the main loadings on Principal Component 1 of
312 the overall genetic variation across treatments suggesting a major role in the evolutionary
313 response irrespective of the amount of migration (**Supplementary Figure 8).** Evolutionary
314 parallelism was not restricted to single sites of standing genetic variation, but was also
315 observed for novel mutations at the gene level. 140 genes significantly enriched in GO-terms
316 for cell-cell adhesion (flocculation and agglutination), polysaccharide catabolic process and
317 cell cycle regulation were hit by multiple novel mutations (up to 187 variants per gene,
318 **Supplementary Figure 9 and Supplementary Table 3**). Cell adhesion traits can increase
319 cluster formation, which might increase settling speed [38] or improve sexual reproduction.
320 Most of the genetic variants, however, did not reach fixation, which may be attributed to
321 genetic redundancy, size effect distribution, negative epistasis, antagonistic pleiotropy or
322 balancing selection [39,40].

323 A single genetic variant that is beneficial in one environment can be beneficial, neutral
324 (conditional neutrality) [41,23,42] or deleterious (antagonistic pleiotropy) [43,44] in another
325 environment. Under conditions of gene flow, allele frequency differences between
326 populations are more likely to be maintained under antagonistic pleiotropy [45]. Additionally, if
327 several loci are subject to antagonistic pleiotropy, linkage disequilibrium can arise even in the
328 absence of epistasis and form the basis for reproductive isolation [46,47]. Even though our pool-
329 seq data does not provide haplotype information, we found evidence for multilocus

330 antagonistic pleiotropy of closely linked loci (**Extended Data Fig. 10**), which appears to
331 commonly arise under divergent selection [6,42,44]. The strongest and most consistent allelic
332 differentiation caused by the ecological selection regime was found for a neighbouring pair of
333 mutations on chromosome II (22kb distance) in the genes *rep2* (variant II:1718756_A; early
334 stop C178*) and *byr2* (variant II:1741521_T; amino acid substitution I259N) in the α genetic
335 background. Both genes are involved in cell cycle regulation, either during mitotic (*rep2*) or
336 meiotic (*byr2*) reproduction. The derived allele for *rep2* had consistently elevated frequencies
337 in allopatric bottom populations relative to the ancestral α population (p_{rep2}=0.5), but reduced
338 frequencies in top populations (p_{byr2}=0.2). The derived *byr2* allele showed the opposite
339 pattern. Not a single replicate population showed simultaneous positive selection of both
340 derived alleles (grey area in **Figure 4a**). With the exception of two local mating populations
341 this held true across migration treatments (**Supplementary Figure 10)**. Moreover, we
342 observed no incidence where the sum of the derived allele frequencies of both loci would
343 exceed a value of 1, which would provide unequivocal evidence for coupling of derived
344 mutations in one haplotype (diagonal line in **Figure 4**). Deterministic simulations further
345 supported opposite directional selection of both loci, as opposed to a scenario of selection on
346 one locus and hitchhiking of a neutral linked variant (see **Methods** and **Supplementary**
347 **Figures 11**). Overall, these results provide evidence for multilocus antagonistic pleiotropy of
348 two derived mutations being favoured in opposite environments (**Figures 4b and 4c**).

349 In the β background, a pair of loci with comparable dynamics was found within a single gene,
350 *msa1*, with the variants I:2319886_T (W106*; high frequency in bottom populations;) and
351 I:2319922_T (W118*; high frequency in top populations) each introducing an early stop
352 codon (**Supplementary Figures 12 & 13**). Similar to *byr2*, wild type *msa1* suppresses
353 sporulation. Evidence of antagonistic pleiotropy is rare in natural populations, but is expected
354 to favour local adaptation and reproductive isolation [45]. The occurrence of several tightly

355 linked loci showing antagonistic pleiotropy (e.g. locked in an inversion [48]) is of particular
356 interest in the context of speciation, as the joint effects of multiple loci increase the potential
357 for coupling of these effects, inducing reproductive isolation [47,49].

358 Summary and Conclusion

359 This study provides experimentally controlled, empirical insight into the effect of migration
360 on adaptive divergence. Parallel divergence was readily achieved in isolation as expected
361 under opposing directional selection [11], mostly from standing genetic variation. Intermediate
362 levels of homogenizing gene flow reduced divergence, but the occupied trait space and
363 genetic variation between population pairs encompassed the full range of locally adapted
364 allopatric populations [10,50]. Contrary to theoretical expectations and previous empirical
365 findings [19,51,52], this included the local mating treatment where sexual reproduction was
366 matched by environment expected to act as a source of premating isolation. Moreover, in
367 contrast to many studies in natural systems, we also did not observe intermediate divergence
368 at intermediate levels of migration (isolation-by-distance and isolation-by-ecology
369 relationships) [8,17,22,53,54]. This is likely owing to the combination of short divergence time and
370 rather high levels of migration (even in parapatry) and the near-absence of genetic drift in our
371 experimental setup. Complementary experiments[23] or sampling of natural populations across
372 a finer-scale of intermediate migration levels [18,55,56] are thus highly encouraged.

373 Contrary to the parapatric and local mating treatment, adaptive divergence was apparent under
374 maximal levels of migration. This is a puzzling observation running counter to the general
375 expectation of an inverse relationship between gene flow and divergence [14]. Under conditions
376 of high gene flow adaptive divergence implies emergence of (quasi-)stable co-existence of
377 distinct strategies allowing exploitation of different niche space [23]. Independent accumulation
378 of mutations promoting further divergence then constitutes the basis, though no guarantee, for
379 ecological speciation[19]. The general expectation, however, is that high levels of gene flow

380 may promote the evolution of an ecological generalist gradually taking over the population
381 without promoting population divergence [57–59,34,60]. Under the latter scenario, the
382 polymorphism observed in the sympatric treatment might be the result of directional selection
383 for a generalist strategy which has not yet reached fixation during the course of 53 sexual
384 generations. Results from several replicates of β sympatric populations are possibly consistent
385 with this scenario. In the vast majority of replicate populations from the α background,
386 however, several lines of evidence support the evolution of true adaptive divergence in
387 sympatry where the pervasive negative correlation and the evolvability of genetic correlations
388 appear to be key. In addition to the evolution of an ecological generalist with high survival in
389 both environments, the strong trade-off with asexual growth additionally promoted the
390 emergence of a second strategy specializing on performance during asexual growth (**Figure**
391 **2**). As a consequence, multivariate phenotypic divergence integrating across life history
392 components reached levels comparable to allopatric populations and exceeded those of
393 parapatry and local mating. At the genetic level, a consistent increase of functional genetic
394 variation (D_a) between ecotypes across nearly all α sympatric populations, but few of the local
395 mating populations sharing the same ancestor, lends further support to the parallel existence
396 of distinct adaptive types independently accumulating mutations. At the current stage, we are
397 ignorant about the long-term stability of these types. However, the fact that they repeatedly
398 evolved and could be observed in nearly all sympatric populations (including several
399 populations of the β background) speaks against a transitory sweep pushing a single,
400 generalist strategy to dominate. Moreover, the relatively large shift in allele frequencies
401 observed in sympatric populations after two rounds of directional selection (**Extended Data**
402 **Fig. 8**) is difficult to reconcile with a transitory sweep and rather suggests maintenance of
403 polymorphism by divergent selection.

404 Stable co-existence of both strategies may be achieved by two non-exclusive mechanisms: (i)
405 by assortative mating facilitated by the evolution of self-compatibility (observed in our
406 experimental setup [61]) or temporal asynchrony in sporulation as anecdotally observed for a
407 subset of populations; (ii) by antagonistic pleiotropy of large effect genes or strong negative
408 epistasis of alleles coding for different life history components [62–65]. Regardless of the precise
409 mechanism, this result overall exemplifies the importance of genetic correlations for
410 inhibiting or enabling adaptive divergence with gene flow, an aspect that may deserve more
411 attention both from a theoretical viewpoint [12,13], as well as in empirical studies of natural
412 systems [20,25].

413 Consistent with contributions of several fitness components to adaptive divergence the
414 underlying genetic basis was polygenic [25]. In line with theoretical predictions [66,67] and existing
415 empirical studies [39], effect sizes from standing genetic variation were skewed with only a
416 small, repeated fraction of genes showing large effects on population differentiation. This was
417 most pronounced in allopatry, where parallel allele frequency shifts of standing genetic
418 variation governed adaptation. In sympatry, populations were near-exclusively characterized
419 by standing genetic variation of allopatric bottom populations. We speculate that this
420 similarity may help explain why diversification more readily occurred in the sympatric
421 migration treatment. Assuming initially stronger selection in the bottom environment the high
422 degree of gene flow might have moved much of the population towards a single (bottom)
423 strategy increasing local competition and opening the opportunity for a top specialist to
424 invade [16]. In the intermediate treatments, a generalist strategy might have been maintained
425 inhibiting the evolution of a specialist strategy. Divergence in sympatry requires the
426 emergence of novel mutations conferring the necessary variation promoting concurrent
427 evolution of an ecological generalist and a growth specialist. This is consistent with our
428 observation of a multitude of unique, novel mutations which were, however, concentrated in

429 specific genes and functional pathways. As a consequence, evolutionary trajectories may be
430 partly predictable, not only at the phenotypic level, but also at the level of the underlying
431 genes [68,69]. Future work unravelling the genotype-fitness map will be necessary to understand
432 the genetic architecture of the opposing adaptive strategies and their trade-offs.

433 Concluding, this evolve-and-resequence experiment demonstrates that divergent selection
434 readily promotes adaptive divergence of ecological specialists in the absence of migration and
435 facilitates the evolution of ecological generalists under conditions of gene flow. Importantly,
436 it further provides evidence that adaptive divergence is also possible, if not favoured, under
437 maximal levels of migration, whereby the evolution of genetic correlations of fitness
438 components appears to play a vital role. The genetic basis of divergence was conferred by a
439 large number of genes exploiting both standing genetic variation in major effect genes with
440 evidence for antagonistic pleiotropy and novel mutations enriched in certain genes and
441 metabolic pathways. These findings contribute to our understanding of the fundamental
442 processes governing adaptation and have potential implications for speciation research,
443 pathogen evolution, pest control or conservation biology.

444 Methods

445 Ancestral populations

446 The preparation of the α and β ancestral populations started with four isogenic strains
447 (parental strains: P1, P2, P5, P6) derived from the Leupold's 968 accession [70]. These four
448 parental strains differed in 14-22 genetic variants (**Supplementary figure 14**) including
449 mutations in the *ade6* gene used as colour marker (*ade6-M216* allele in P1 and P5, and the
450 *ade6-M210* allele in P2 and P6), and the homothallic mating locus with configuration h^{-S}
451 (in P2 and P5) or h^{+S} ((in P1 and P6 [71]). These strains are obligatory outcrossing
452 (heterothallic), although along the experiment we observed the emergence of homothallic

453 phenotypes (mating type switching), [61]. In general, unless specified, asexual growth was
454 performed in standard liquid Edinburgh Minimal Medium (EMM; Per liter: Potassium
455 Hydrogen Phthalate 3.0 g, Na $HPO_4 \cdot 2H_2O$ 2.76 g, NH_4Cl 5.0 g, D-glucose 20 g, $MgCl_2 \cdot 6H_2O$
456 1.05 g, $CaCl_2 \cdot 2H2O$ 14.7 mg, KCl 1 g, Na_2SO_4 40 mg, Vitamin Stock ×1000 1.0 ml, Mineral
457 Stock ×10,000 0.1 ml [72]). Sexual reproduction took place on 2% agar solid Pombe Minimal
458 Glutamate medium (PMG corresponding to EMM medium substituting ammonium chloride
459 by 5 g l^{-1} glutamic acid). Ecological selection was conducted in Selection Medium (SM; as
460 PMG with glutamic acid reduced to 0.8 g l^{-1}). In all cases, media was supplemented with
461 100 mg l^{-1} adenine.

462 Preparing the ancestral populations for the experiment involved two phases. In the first phase
463 (*phase I*), settling speed at stationary phase was used as ecological contrast resulting in
464 disruptive selection on a complex trait involving growth rate, cell size and cell morphology [38]
465 (**Supplementary Figure 15**). The aim of *phase I* was to induce genetic variation relevant to
466 ecological specialization for fast or slow settling rate (bottom and top selection regime,
467 respectively) in independent, asexually reproducing populations. In total, we maintained 24
468 populations (6 populations per parental strain), 12 for fast settling (bottom selection) and 12
469 for slow settling (top selection). The experiment was performed in cycles of asexual growth in
470 5 ml of EMM at 32°C shaking at 250 rpm for two days, followed by a selection step where
471 1% of the cells were transferred to fresh medium (around 5 million cells were transferred).
472 For bottom selection, 1 ml of saturated media were placed on the top of a column with 10 ml
473 of SM. The column was centrifuged for 45 seconds at 100 g, and 300µl from the bottom
474 fraction of the column were collected. For top selection, the saturated medium was diluted to
475 a final volume of 15ml with water, and centrifuged for 2 minutes and 45 sec at 100 g, after
476 which 500 µl of the surface liquid was collected. Collected bottom and top fractions were then
477 placed in 5 ml of fresh EMM media for each population to start a new cycle. In total, we

478 conducted 50 and 62 selection cycles for bottom and top selection, respectively,
479 corresponding to approximately 430 and 530 asexual generations. At the end of this phase,
480 each of the 24 evolved populations was diluted and plated in solid EMM with 2% agar. Plates
481 were grown for three days and one single colony was isolated from each population (one
482 isogenic strain per evolved population) to initiate the second phase (*phase II*).

483 Since the *phase I* was run only using asexual cycles, during *phase II*, the aim was to add
484 sexual reproduction to the cycles and increase reproductive efficiency, while maintaining
485 variability in the ecological selection regime (top and bottom selection) produced in *phase I.*
486 *Phase II* was started in duplicate maintaining the identity of the colour marker using the
487 strains derived from evolved populations from *phase I* with parental P2 and P6 ancestry
488 (*ade6-M210* allele, or *α* genetic background) or from parent P1 and P5 (*ade6-M216* allele, or
489 *β* genetic background). Each of the 24 evolved strains were grown to saturation in EMM, and
490 within the α and β genetic background the six Plus mating types were each mixed in equal
491 proportion to each of the six Minus mating types for all possible combinations, and thereafter
492 transferred to mating plates. After three days of mating on solid PMG, 1% of the cells were
493 harvested from each cross, sexually produced offspring (ascospores) were isolated by killing
494 all non-mated cells using Glusulase (0.5% v/v overnight; PerkinElmer) followed by a 30%
495 ethanol treatment for 30 minutes. Spores were recovered and incubated in 5ml of EMM at
496 32°C for two days. A second round of mating was performed, now mixing all offspring per
497 genetic background from the first round resulting in two population pools (α and β). For each
498 pool ten independent replicate populations were propagated for 20 cycles of disruptive
499 selection described above with the addition of sexual reproduction after the selection step
500 (**Supplementary Figure 16**). Sexual reproduction was introduced in two ways: in half of the
501 populations (five each α and β) cells were mixed prior to sexual reproduction, and in the
502 remaining populations mating was performed independently in each of the selection fractions

503 (bottom or top) where after spores were mixed in equal proportions. In both treatments spores
504 were harvested to remove un-mated cells by glusulase and ethanol treatment as described
505 above and were used to start the new cycle. *Phase II* was run for 20 cycles, each lasting six
506 days. After 20 sexual generations, the 10 evolved populations from each ancestral α or β
507 population were mixed to produce two independent populations with different genetic
508 background and different composition of standing variation. These populations were used to
509 start the experiment forming the basis of this study. They are referred to (α and β) ancestral
510 populations.

511

512 Experimental evolution: divergent selection with migration

513 The evolutionary experiment was run in duplicate using both ancestral population (α or β
514 populations from end of *phase II*). For each background, we ran 66 replicate populations
515 corresponding to four treatments varying in the level of migration (see below). All steps of the
516 experiment were performed in 96-well plates, either 1.2ml deep-well plates for asexual
517 growth and ecological selection, or flat bottom 360 µl microtiter plates for sexual
518 reproduction. Similar to preparation *phase II* the experiment was run in six day cycles, each
519 including growth, ecological selection and sexual reproduction. Experimental conditions were
520 modified to accommodate larger numbers of replicates and introduce four levels of migration.
521 Populations were grown asexually for two days in 300 µl of EMM per population followed by
522 ecological selection. For bottom selection, 50 µl of cells were placed on the top of a column
523 with 750 µl of SM in a 96 deep-well plate. After 9 minutes, 25 µl of the bottom fraction was
524 collected (corresponding to 0.5 % of cells, or around 150,000 cells). For top selection, 100 µl
525 of cells were placed on the top of a column with 550 µl of SM in a 96-well plate. This plate
526 was centrifuged at 100 rcf (705 rpm) for two minutes and 45 seconds, and 25 µl were

527 collected from the surface (again corresponding to 0.5 % of cells, or around 150,000 cells).
528 The subsequent step of sexual reproduction was performed in microtiter plates with 150 µl of
529 PMG per well. After three days, 25% of the sexually produced offspring (ascospores) were
530 harvested by killing all non-mated cells using Glusulase (digestive enzyme mixture) in the
531 incubator at 27.5 ^{o}C overnight, followed by 30% ethanol treatment for 30 minutes. These
532 spores were used to start the next cycle.

533 For each background, we modified the amount of migration between ecologically selected
534 populations (top and bottom fraction after selection) in four treatments (**Figure 1 and**
535 **Supplementary Figure 1**). i) In the *allopatric* treatment, half of the populations were
536 subjected to bottom selection, and half to top selection. Sexual reproduction was restricted to
537 within each population. ii) In the *parapatric* treatment, replicates were divided into non-
538 independent population pairs experiencing opposite ecological selection (top or bottom
539 selection). After selection, 5% of the selected cells were reciprocally transferred between
540 populations of each pair. Sexual reproduction occurred independently in each population. iii)
541 In the *local mating* treatment, independent populations were grown asexually and experienced
542 disruptive selection for both, top and bottom selection. Sexual reproduction occurred in each
543 resulting fraction independently. The spores produced from top and bottom mating plates
544 were then mixed and transferred together for asexual growth. iv) In the s*ympatric* treatment,
545 independent populations were grown asexually and experienced disruptive selection for top
546 and bottom selection. Prior to sexual reproduction the two fractions were fully mixed,
547 transferred to a mating plate and the resulting spores were used again for asexual growth.

548 Each treatment contained 22 replicates of evolving populations (sympatry and local mating
549 treatment) or pairs of populations (allopatry and parapatry) giving a total of 66 replicate
550 populations for each ancestral background, or 132 altogether. In order to maintain the same
551 population mutation rate ($N_e\mu$) in all treatments, population size was matched during asexual

552 growth performed in two independent wells per population for the sympatric and local mating
553 treatments, which were then mixed after growth before selection. Additionally, the sexual
554 reproduction step for the sympatric treatment was performed in two wells per population. In
555 order to control for cross contamination between populations, we included two empty wells
556 per treatment, with media, but without cells. The experiment was run in total for 53 cycles (53
557 cycles of sexual reproduction and around 700 asexual generations).

558 During the entire experiment, populations were stored every three cycles after asexual growth
559 in YES medium with 15 % glycerol, and were cryopreserved at -80°C.

560

561 ## Fitness measurements

562 We measured fitness of the evolved populations relative to the ancestral populations (α and β
563 ancestral populations after the two preparation phases) for four fitness components: asexual
564 growth, sexual reproduction and survival of ecological selection for top or bottom.
565 Additionally, in order to identify the potential for differentiation within populations
566 (subpopulations - population structure), each population was subjected to two experimental
567 cycles removing migration (as in allopatric treatment). This resulted in a top and bottom
568 subpopulation. To ensure comparability across treatments the two additional cycles were
569 performed prior to fitness measurement in all four treatments. To quantify relative fitness, we
570 performed a competition assay between all evolved populations and ancestral populations
571 (test populations) using a fluorescent isogenic strain as intermediary reference. The reference
572 fluorescent strain was derived from the lab strain Leupold's 968 $h^{90\ 70}$ containing an
573 introduced mCherry-marker (strain EBC47 described in[61]). Each test population and reference
574 fluorescent strain was first grown independently to saturation for two days. Subsequently, 250
575 µl of the test population were mixed with 100 µl of the reference (mix before growth - BG).

576 10 µl of the mix were then diluted with 100 µl of water and the frequency of fluorescent
577 (reference strain) vs. no-fluorescent cells (from the test population) were measured using a
578 flow cytometer (BD LSR Fortessa, at the Core Facility Flow Cytometry, LMU) (baseline
579 frequency before growth – f_{BG}). A fraction of 5 µl (BG) was then mixed with 500 µl of SM
580 (selection media) of which 30 µl were transferred to 100 µl of EMM. After 24 h of asexual
581 growth, the change in frequency was measured using the flow cytometer (frequency after
582 growth – f_{AG}) providing an estimate of growth rate differences between the test population
583 and the reference. Another fraction of 50 µl (BG) was subjected to one cycle of bottom
584 selection. Given the reduced number of cells for measurements after selection, the selected
585 fraction was mixed with 100 µl of EMM and grown for 24 hours. After growth, the change in
586 frequency was measured using the flow cytometer (frequency after bottom selection plus
587 growth – f_{BSG}). A third fraction of 100 µl (BG) was placed on the top of a top selection
588 column, and a cycle of top selection was performed. The selected fraction was grown and
589 measured as for bottom selection described above (frequency after top selection and growth –
590 f_{TSG}). To measure sexual reproductive success, 20 µl of the reference strain and 80 µl of the
591 test population were mixed, and the fluorescent and non-fluorescent proportion of this mix
592 was measured in the flow cytometer (frequency before mating - f_{BM}). To reproduce the
593 evolutionary environment, 10 µl of the mix was diluted to 1,000 µl of SM of which 25 µl was
594 transferred to a PMG mating plate. After three days of sexual reproduction, spores were
595 harvested as in the experiment and transferred to 100 µl of EMM for asexual growth. After 24
596 hours, samples were measured in the flow cytometer (frequency after mating and growth –
597 f_{AMG}). Eight technical replicates were performed for each fitness component measurement and
598 population. Raw data was converted using flowCore 1.11.20 (Ellis et al. 2009) and analysed
599 in R. Debris was filtered by gating in FSC width and height and a cut-off in the mCherry

signal was used to define reference and focal populations (see **Supplementary Figure 17** for representative example).

All fitness components were measured relative to the reference fluorescent strain. Due to technical limitations, measurements required a growth step after selection and after sexual reproduction. To compensate for these steps, we used the calculations described below, to obtain fitness estimates of the evolved populations relative to the (α or β) ancestral population of the experiment (adaptation). First, we estimated the number of asexual generations for the reference fluorescent strain in 24 hours to be around 6. Given an initial frequency of cells before growth (f_{BG}) for both evolved population and reference strain, as well as the frequency after growth (f_{AG}), we inferred the number of reference cells after 24 hours of growth as:

$$N_{refAG} = N_{refBG} * e^{t*M_{ref}}$$

Where $t = 6$ and $M_{ref} = 1$ (Malthusian parameter of the reference strain was set to 1). The number of cells of the evolved populations is:

$$N_{evolAG} = \frac{f_{AG} * N_{refAG}}{1 - f_{AG}}$$

Then the number of evolved cells before and after growth were used to calculate a Malthusian growth parameter for the evolved population as:

$$M_{evol} = \frac{log(N_{evolAG}/N_{evolBG})}{t}$$

The same calculation was used to estimate a Malthusian parameter per cell division for the ancestral populations ($M_{ancestral}$). The relative fitness for growth (g) then is:

$$\frac{N_{evol}}{N_{ancestral}} = \frac{e^{tM_{evol}}}{e^{tM_{ancestral}}}$$

616 The relative fitness after ecological selection (top or bottoms selection), was calculated in the
617 same way in both cases. We used the calculated M_{evol} parameter to differentiate the change in
618 frequency by selection (frequency after top or bottom selection – f_{TS} or f_{BS}) from the change
619 from selection plus growth (f_{TSG} and f_{BSG} described above). For that, we calculated the number
620 of reference cells remaining after top and bottom selection alone from saturated medium
621 (Expected_pS_{ref}), and used it to calculate the number of reference cells after selection in the
622 mix:

$$N_{refBS} = N_{ref}Saturation * DilutionFactorMix * \text{ Expected\_p}S_{ref}$$

623 As the fraction after selection was measured after a step of asexual growth of 24 hours, N_{refBS}
624 was used to calculate the number of reference cells after selection and growth (N_{refBSG} and
625 N_{refTSG}) with $M_{ref} = 1$ as:

$$N_{refBSG} = N_{refBS} * e^{6*M_{ref}}$$

626 As before, using initial densities and the frequency before selection we calculated the number
627 of evolved cells before selection (N_{evolBG}) as:

$$N_{evolBG} = \frac{BG * N_{refBG}}{1 - BG}$$

628 And the number of cells after selection without growth as:

$$N_{evolBS} = \frac{f_{BSG} * N_{refBSG}}{(1 - f_{BSG}) * e^{6*M_{evol}}}$$

629 The relative fitness for ecological selection (W) was then calculated as:

$$RelativeW = \frac{N_{evolBS}/N_{evolBG}}{N_{refBS}/N_{refBG}}$$

630 The fitness relative to the reference was calculated for evolved and ancestral populations, and
631 the final relative fitness with respect to ancestral populations was calculated as the ratio
632 between them.

633 Relative fitness of sexual reproduction was estimated similarly. As the measurements of
634 sexual reproduction efficiency were inferred after a period of 24 hours of asexual growth
635 (AMG), frequencies after mating were corrected using M_{evol} (frequency after mating without
636 growth – f_{AM}). Then values of sexual reproduction efficiency of the test population relative to
637 the reference was calculated as:

$$Relative\_r = \frac{f_{AM} * N_{refBM}}{N_{evolBM} * (1 - f_{AM})}$$

638 Note that the measure *r* is an aggregate of mating, sporulation and germination efficiency. We
639 assume that the fluorescent marker in the reference strain follows Mendelian inheritance and
640 that the effect of mating between evolved and reference cells is on average equal for the
641 offspring with and without the fluorescent marker.

642 Estimates of relative growth rate (g), response to selection for top or bottom (W_T or W_B,
643 respectively), and the efficiency of sexual reproduction (r) constitute fitness components that
644 were compared between migration treatments and selection regimes. For each fitness
645 component (ratio data) a log transformation was performed to obtain a normal distribution to
646 which a generalised linear model was fitted using treatment and selection regime as fixed
647 variables and population and technical replicate as random factors. To correct for occasional
648 outliers due to experimental error, for each population, the replicate that deviated most from
649 the median was discarded. In this model, treatments were contrasted to allopatric populations
650 (**Supplementary Table 1 & 2**). In addition, we performed Principal Component Analyses
651 (PCA): i) including all treatments and ii) separately per treatment, using z-score normalized

652 values for the log transformed fitness values per fitness component and visualised using the R
653 package *factoextra* v3.4.4 [73]; PCAs were conducted for each ancestral genetic background
654 separately, using all variants (**Fig. 3**) or only ancestral variation (**Extended Data Fig. 4**). We
655 further calculated correlation matrices of all four fitness components for each treatment and
656 genetic background using standardized z-transformed fitness values. Calculations included all
657 22 populations (allopatry, parapatry) or subpopulations (local mating, sympatry).
658 **Supplementary Figure 18** shows the correlation for allopatry and sympatry in the α
659 background. The sign of the slope of the lines between points – connecting the pairs of
660 subpopulations in sympatry derived from the same population – indicate if the correlation
661 observed among populations is maintained within populations.

662

663 Genomic data generation and pre-processing

664 Genetic analyses were performed in all populations obtained during the preparation of the
665 ancestral populations (*phase I* and *II*), the two ancestral populations (α, β), all evolved
666 populations, and subtractions from the local mating and sympatry treatments after two cycles
667 of selection without migration. Specifically, genomic DNA was extracted from the following
668 populations/strains: the four parental strains (P1, P2, P5 and P6), the 24 evolved strains of
669 *phase I*, the two ancestral populations starting *phase II*, the two ancestral populations starting
670 the experiment (α and β ancestors), the 132 evolved populations at the end of the experiment,
671 and 44 samples corresponding to top and bottom fractions from local mating and sympatric
672 populations. Genomic DNA was extracted using Zymo Research Quick-DNA™
673 Fungal/Bacterial 96 Kits according to the manufacturers' instructions. Library preparation and
674 Illumina HiSeqX, paired-end 150 bp read length, v2.5 sequencing chemistry, was performed
675 at the SNP&SEQ platform of the SciLifeLab at Uppsala University. Libraries were prepared

676 from 1 μg DNA using the TruSeq PCRfree DNA sample preparation kit, targeting an insert
677 size of 350 bp. For sequencing, 48 libraries with barcodes were pooled per lane randomized
678 across treatments. Samples were sequenced to sequence coverage over above 200 x
679 (**Supplementary Figure 19**). Raw sequencing data is available at the National Center for
680 Biotechnology Information (NCBI) under Bioproject ID PRJNA604890.

681 Adaptors were removed from raw reads using *cutadapt 1.3* [74], read-pairs were filtered and
682 trimmed by quality using *trimmomatic 0.32* [75] and *FastQC 0.11.5*. Filtered reads were then
683 mapped to the reference genome (ASM294v2 [76]) using *BWA 0.7.15*[77]. Local realignment was
684 performed using *GATK 3.3.0* [78] and the Picard toolkit *picard 1.92*
685 (https://broadinstitute.github.io/picard/). Genetic variants and frequencies (both SNPs and
686 small indels) were inferred using the package *VarScan 2.3.7* [79], with minimum mapping
687 quality of 30 and a threshold p-value of $1x10^{-4}$. Variants were filtered to exclude 1) variants
688 with more than 90% of the reads supported by a single strand; 2) variants with coverage lower
689 than 10% of genome-wide average or higher than 1.3 times the estimated maximum coverage
690 as suggested by Heng[80]; 3) variants falling into repetitive regions identified using
691 *RepeatMasker 4.0.7* (http://repeatmasker.org). Genetic variants were annotated relative to the
692 reference genome using *SnpEff 4.3*[81]. Based on the annotation for effect on the closest
693 genomic region, genetic variants were classified according to the predicted size effect into
694 four, mutually exclusive categories as defined in *SnpEff 4.3*: i) *modifier*, including non-coding
695 transcript exon variant, intragenic region, intron variant, 5' UTR variants and 3' UTR
696 variants; ii) *low*, including synonymous, splice region variants, splice region variant and 5'
697 UTR premature start codon gain variant; iii) *moderate*, including missense variants, disruptive
698 in-frame deletion and insertion, and conservative in-frame insertion; and iv) *high*, including
699 stop-gain, start-loss and frame-shift variant. Coverage values per base were calculated using
700 *SAMtools* 1.9 [77]. Gene function and phenotype effect for variants that showed strong

701 divergent selection or were hit multiple times independently were checked at pombase.org [82].
702 Gene ontology analysis for enrichment was performed using Fisher's exact test for the
703 annotations of biological process from pombase.org, using false discovery rate as correction.

704

705 Decomposition of genetic and fitness variation

706 Allele frequencies were used to calculate population genetic parameters including average
707 number of pairwise differences between populations (D_{xy}[83]) and the expected genetic variance
708 within populations relative to the total expected genetic variance (F_{st}[84]) using custom scripts.
709 Population allele frequencies were further used to perform PCAs, which were visualised using
710 the R package *factoextra* v3.4.4. Analyses were conducted for all populations per genetic
711 background (α or β; **Extended Data Fig. 4**) and by treatment always including the allopatric
712 populations as point of reference (**Figure 3**). This analysis was performed for all mutations
713 (**Figure 3** and **Extended Data Fig. 4a**), or only for variants present in the α or β ancestral
714 populations (standing variation; **Extended Data Fig. 4b**).

715 We then explored the relationship between genetic variation and variation in fitness
716 components. We extracted the two major axes of variation (PC1 and PC2) for genetic
717 variation (**Figure 3** and **Extended Data Fig. 4**) and for variation in the log normalized
718 relative fitness values across all four fitness components (**Extended Data Fig. 2**) and
719 investigated the association using a linear model using the *stats v3.6.0* package. The analysis
720 was done independently for each genetic background and treatment excluding sympatry and
721 the local mating treatments due to the lack of correspondence between sequencing data (from
722 population pools) and fitness estimates (from selected fractions within population –
723 subpopulations). In the case of parapatric populations, the fitted model additionally included
724 ecological selection regime as fixed variable (top and bottom selection regime).

725 We then evaluated the potential for genetic divergence within populations with high migration
726 (local mating and sympatry). First, allele frequencies were used to calculate ancestral
727 divergence (D_a: difference between D_{xy} and mean π) between the top and bottom fraction per
728 population (**Extended Data Fig. 7**) using custom scripts. Then we compared allele frequency
729 changes between whole pool samples and their respective top and bottom fractions (see
730 examples in **Supplementary Figure 3**). For each population we counted the proportion and
731 number of genetic variants with allele frequency change higher than 0.2 in the comparisons:
732 top – bottom fraction, pool – top, and pool – bottom (**Supplementary Figure 4**). The change
733 of frequency of 0.2 since allele frequency changes higher than 0.15 are not expected for
734 neutral genetic variation (see individual based simulation below), but a lower threshold of 0.1
735 gave similar qualitative results. Dominant fractions were compared between treatments (local
736 mating and sympatry) and genetic backgrounds (**Extended Data Fig. 8**). Significance of the
737 difference between groups were tested using a quasibinomial model in a nested generalised
738 lineal model with treatment and fraction as fixed variables and population as random factors.

739

740 Individual based forward simulations

741 In order to identify the expected allele frequency distribution of neutral genetic variants and
742 the effect of physical linkage we performed individual based forward simulations using *SLiM*
743 *3.2.1* [85]. We contrasted simulations including only neutral variants to simulations including
744 both neutral and selected variants We parameterized the simulations with estimates from the
745 literature including a mutation rate of $2 \cdot 10^{-10}$ site^{-1} generation^{-1} [86], an average recombination
746 rate of $1 \cdot 10^{6}$ site^{-1} generation^{-1} [87], and a cloning rate of 0.90 generation^{-1} (equivalent to around
747 1 sexual cycle every 18 asexual generations). We simulated genetic variation for one
748 chromosome of 1 Mb in size for allopatric populations in cycles following the setup of the

749 experiment (**Figure 1**). $3 \cdot 10^5$ haploid individuals (cells) grew asexually to a saturation point
750 of $3 \cdot 10^7$ individuals. Growth was followed by a selection step reducing population size to
751 $3 \cdot 10^5$, subsequently undergoing a cycle of sexual reproduction with an outcrossing rate of
752 0.90 generation^{-1}. The resulting offspring re-started the cycle. Simulations were run for 800
753 asexual generations (corresponding approximately to 700 asexual generations during 53
754 experimental cycles), 1,000 generations (mimicking *phase II* + experiment) and 2,000
755 generations to explore longer-term evolutionary dynamics. In order to reduce the
756 computational effort, all parameters were scaled relative to an effective population size N_e of
757 $3 \cdot 10^3$ as suggested in the *SLiM* manual. Simulations were run first including only neutral
758 variants (**Supplementary Figure 5**) and then adding selected variants (**Supplementary**
759 **Figure 6**). For selected variants, we included a range of parameters specifying: 1) the
760 proportion of emerging selected variants relative to neutral variants (from 100 to 10000
761 neutral variants per selected variant) and 2) selection coefficients which were sampled from
762 an exponential distribution with varying mean (from 0.01 to 0.1). For each parameter
763 combination, we ran 100 replicate simulations and report the mean tabulated number of
764 genetic variants per allele frequency across simulations. Neutral variants alone did not reach
765 allele frequencies higher than around 0.3 after 2000 generations, and only reached 0.12 in 800
766 generations (**Supplementary Figure 5**). In the presence of linked selected variants, mean
767 allele frequencies of neutral variants increased, but only under conditions of high selection
768 coefficients and a low occurrence of selected relative to neutral variants (**Supplementary**
769 **Figure 6**).

770

Allelic differentiation by ecological contrast

To test for the difference in allele frequency per variant between ecologically contrasting conditions (allopatric top and bottom regime) we used a logistic regression with binomial and quasibinomial error structure taking over-dispersion into account. In general, the quasibinomial model is not appropriate for cases when variants were only found in some populations (new mutations in the last phase of the experiment), even when derived allele frequencies clearly differed between top and bottom selected populations where present. For example, variants found in high frequency in ~5 populations, but not present in all bottom populations, where not found to be significantly different in the quasibinomial model. For variants present in all population (standing genetic variation), the quasibinomial model appeared more appropriate.

Forward simulations for linkage disequilibrium between potentially adaptive loci

This analysis was performed for pairs of genetic variants showing signatures of antagonistic pleiotropy for disruptive adaptation to ecological selection for top or bottom in allopatric populations. This included variants *II:1718756* (with the derived allele A in high frequency in bottom populations relative to the reference allele present in high frequency in top populations) and *II:1741521* (derived allele T in high frequency in top populations relative to reference allele in high frequency in bottom populations). These two loci were identified in populations with the α genetic background, located 22,765 bp apart. For populations derived from the β genetic background, we performed the same analysis on variants *I:2319886* (with the derived allele T in high frequency in bottom populations relative to the reference allele present in high frequency in top populations) and *I:2319922* (derived allele T in high

795 frequency in top populations relative to reference allele in high frequency in bottom
796 populations). This second pair of loci was 36 bp a part.

797 Given the close physical proximity between these pairs of variants, the strong correlation in
798 allele frequency of variants could be due to ecologically mediated selection acting 1) on both
799 variants either in the opposite or same direction generating linkage disequilibrium (hypothesis
800 1), or 2) on only one of the two variants dragging along a physically linked neutral locus
801 (hypothesis 2).

802 Sequencing of population pools did not allow haplotype inference. Yet, the initial allele
803 frequencies of both loci in the ancestral populations restrict the range of possible initial
804 haplotype frequencies. In the ancestral α population, we observed an allele frequency of 0.5
805 and 0.2 for the derived alleles *II:1718756_A* and *II:1741521_T,* respectively (or 0.5 and 0.8
806 for the reference alleles). We ran deterministic simulations under hypothesis 2 where only one
807 of the locus was under selection. In the first case, the variant *II:1718756* was under selection
808 (A allele being beneficial under bottom selection) and the other locus *II:1741521* was neutral.
809 The initial frequencies of haplotypes A1B1, A1B2, A2B1, and A2B2 were denoted as X1,
810 X2, X3 and X4. A1 represents the allele under selection (II:1718756_A in this case) with an
811 alternative reference allele A2; B1 and B2 were assumed to be neutral. This translated into a
812 fitness matrix such as ωA1B1 = ωA1B2 = 1 and ωA2B1 = ωA2B2 = 1 - s, where *s* is the
813 selection coefficient. From the fitness matrix, marginal fitness for haplotype (*i*) over other
814 haplotypes (*j*) and mean fitness were calculated for the population as: $\overline{\omega}i = \sum_{j=1}^{4} X_j \omega ij$ and
815 $\overline{\omega} = \sum_{i=1}^{4} X_i \overline{\omega} i$. Initial haplotype frequencies were estimated considering the possible range
816 of values such as: $X1 + X2 = f(A1) = 0.5$, $X1 + X3 = f(B1) = 0.8$, and $X1 + X2 +$
817 $X3 + X4 = 1$. After one cycle of sexual reproduction the change in haplotype follows as:

$$\Delta X1 = \frac{X1(\bar{\omega}1 - \bar{\omega}) - r\omega_{14}D}{\bar{\omega}}, \Delta X2 = \frac{X2(\bar{\omega}2 - \bar{\omega}) - r\omega_{14}D}{\bar{\omega}}, \Delta X3 = \frac{X3(\bar{\omega}3 - \bar{\omega}) - r\omega_{14}D}{\bar{\omega}}, \quad \Delta X4 = \frac{X4(\bar{\omega}4 - \bar{\omega}) - r\omega_{14}D}{\bar{\omega}}$$

where r is the recombination rate (from 0 to 0.5) between the selected and the neutral loci, used also as a measurement of genetic distance, and D is linkage disequilibrium given by: $D = X1X4 - X2X3$. Decrease of D was modelled as a function of r over time: $D' = (1 - r)D$.

This model was used to run simulations with different parameters for X1, r and s. Final allele frequencies for the neutral locus were reported once the selected locus reached fixation (X1 + X2 > 0.999). This was done for both selective regimes, one in which A1 was positively selected (allopatric bottom populations) and another one in which A2 was under positive selection (allopatric top populations). We then considered the opposite case, when the variant conferring a selective advantage was under ecological top selection (allele *II:1741521_T* positively selected in top populations) and the second locus was neutral (*II:1718756*). We compared the predicted range of allele frequencies when variants were assumed to be neutral with observed allele frequencies in the experiment. The prediction is that under physical linkage between a selective and a neutral variant (hypothesis 2), the range of observed allele frequencies should be within the simulated intervals. In the case of disruptive selection of both loci, the range of observed allele frequencies should be larger than in the simulations, since the second selected variant would increase in frequency even after the first one fixed. The same analysis was repeated using the pair of loci from the β populations *I:2319886* and *I:2319922*.

Acknowledgments

We thank S. Lorena Ament-Velásquez, Roger Butlin, Ulrich Knief, Dirk Metzler, Claire Peart, Ricardo Pereira, Rike Stelkens, Matthias Weissensteiner, and members of the Immler and Wolf labs for providing intellectual input on the various analyses, and comments on the manuscript. We are further indebted to Tauseef Ahmad, Gaby Kumpfmüller, Hildegard Lainer and Natalia Zajac for help with laboratory work, Douglas Scofield for bioinformatics support and Ben Haller for support running *SLiM*. We further acknowledge support for genomic data generation from the SNP&SEQ Technology Platform in the National Genomics Infrastructure, Uppsala, Sweden. Flow cytometry was performed at the Core Facility FlowCyt at LMU. The computational infrastructure was provided by the UPPMAX Next-Generation Sequencing Cluster and Storage (UPPNEX) project funded by the Knut and Alice Wallenberg Foundation and the Swedish National Infrastructure for Computing. Funding was provided to JW by LMU Munich, Science of Life Laboratories National Projects and Uppsala University.

Contributions

S.T., B.P.S.N, S.I. and J.B.W.W. conceived the study; S.T., B.P.S.N. and B.W. performed experiments; S.T. and B.W .performed phenotypic measurements. All analyses were performed by S.T. with contributions from B.P.S.N. in phenotypic analyses. S.T. and J.B.W.W. wrote the manuscript with input from B.P.S.N. and S.I..

Competing interests

The authors declare no competing interests.

Data and code availability

All data generated for this study are archived in the sequence read archive under bioproject ID PRJNA604890 at the National Centre of Biotechnology Information

(www.ncbi.nlm.nih.gov/sra). All code used for the analyses, fitness data and a list of genetic variants (.vcf format) is available at https://github.com/EvoBioWolf/SchPom_Exp_AdaptDiv and Zenodo DOI: 10.5281/zenodo.4133489 [88].

References

1. Darwin, C. & Wallace, A. R. On the tendency of species to form varieties; and on the perpetuation of varieties and species by natural means of selection. *J Proc Linn Soc London* 46–50 (1858).
2. Schluter, D. Evidence for Ecological Speciation and Its Alternative. *Science* **323**, 737–741 (2009).
3. Dobzhansky, T. *Genetics and the Origin of Species*. vol. 11 (Columbia university press, 1937).
4. Mayr, E. *Animal Species and Evolution. Animal species and their evolution.* (Harvard University Press; London: Oxford University Press, 1963).
5. Coyne, J. A. & Orr, H. A. *Speciation*. (Sinauer, 2004).
6. Dettman, J. R., Sirjusingh, C., Kohn, L. M. & Anderson, J. B. Incipient speciation by divergent adaptation and antagonistic epistasis in yeast. *Nature* **447**, 585–588 (2007).
7. Haldane, J. B. S. A mathematical theory of natural and artificial selection. (Part VI, Isolation.). *Mathematical Proceedings of the Cambridge Philosophical Society* **26**, 220–230 (1930).
8. Räsänen, K. & Hendry, A. P. Disentangling interactions between adaptive divergence and gene flow when ecology drives diversification. *Ecology Letters* **11**, 624–636 (2008).
9. Smadja, C. M. & Butlin, R. K. A framework for comparing processes of speciation in the presence of gene flow. *Molecular Ecology* **20**, 5123–5140 (2011).
10. Ronce, O. & Kirkpatrick, M. When Sources Become Sinks: Migrational Meltdown in Heterogeneous Habitats. *Evolution* **55**, 1520–1531 (2001).
11. Spichtig, M. & Kawecki, T. J. The maintenance (or not) of polygenic variation by soft selection in heterogeneous environments. *The American Naturalist* **164**, 70–84 (2004).
12. Guillaume, F. & Whitlock, M. C. Effects of migration on the genetic covariance matrix. *Evolution* **61**, 2398–2409 (2007).

887 13. Arnold, S. J., Bürger, R., Hohenlohe, P. A., Ajie, B. C. & Jones, A. G. Understanding the
888 evolution and stability of the G-matrix. *Evolution* **62**, 2451–2461 (2008).
889 14. Garant, D., Forde, S. E. & Hendry, A. P. The multifarious effects of dispersal and gene flow on
890 contemporary adaptation. *Funct Ecol* 1–10 (2006).
891 15. Nosil, P. Speciation with gene flow could be common. *Molecular Ecology* **17**, 2103–2106 (2008).
892 16. Dieckmann, U., Doebeli, M., Metz, J. A. J. & Tautz, D. *Adaptive Speciation*. (Cambridge
893 University Press, 2012).
894 17. Shafer, A. B. A. & Wolf, J. B. W. Widespread evidence for incipient ecological speciation: a
895 meta-analysis of isolation-by-ecology. *Ecology Letters* **16**, 940–950 (2013).
896 18. Hendry, A. P., Bolnick, D. I., Berner, D. & Peichel, C. L. Along the speciation continuum in
897 sticklebacks. *Journal of Fish Biology* **75**, 2000–2036 (2009).
898 19. Nosil, P. *Ecological speciation*. (Oxford University Press, 2012).
899 20. Arnegard, M. E. *et al.* Genetics of ecological divergence during speciation. *Nature* **511**, 307–311
900 (2014).
901 21. Seehausen, O. *et al.* Genomics and the origin of species. *Nature Reviews Genetics* **15**, 176–192
902 (2014).
903 22. Wolf, J. B. W. & Ellegren, H. Making sense of genomic islands of differentiation in light of
904 speciation. *Nature Reviews Genetics* **18**, 87–100 (2017).
905 23. Gray, J. C. & Goddard, M. R. Gene-flow between niches facilitates local adaptation in sexual
906 populations. *Ecology Letters* **15**, 955–962 (2012).
907 24. Soria-Carrasco, V. *et al.* Stick Insect Genomes Reveal Natural Selection's Role in Parallel
908 Speciation. *Science* **344**, 738–742 (2014).
909 25. Schluter, D. Adaptive radiation along genetic lines of least resistance. *Evolution* 1766–1774
910 (1996).
911 26. Reznick, D. The Structure of Guppy Life Histories: The Tradeoff between Growth and
912 Reproduction. *Ecology* **64**, 862–873 (1983).
913 27. Roff, D. A. Trade-offs between growth and reproduction: an analysis of the quantitative genetic
914 evidence. *Journal of Evolutionary Biology* **13**, 434–445 (2000).

915 28. Haselhorst, M. S. H., Edwards, C. E., Rubin, M. J. & Weinig, C. Genetic architecture of life
916 history traits and environment-specific trade-offs. *Molecular Ecology* **20**, 4042–4058 (2011).
917 29. Silva, F. F. G., Slotte, A., Johannessen, A., Kennedy, J. & Kjesbu, O. S. Strategies for partition
918 between body growth and reproductive investment in migratory and stationary populations of
919 spring-spawning Atlantic herring (Clupea harengus L.). *Fisheries Research* **138**, 71–79
920 (2013).
921 30. Lande, R. Quantitative Genetic Analysis of Multivariate Evolution, Applied to Brain: Body Size
922 Allometry. *Evolution* **33**, 402–416 (1979).
923 31. Arnold, S. J. Constraints on Phenotypic Evolution. *The American Naturalist* **140**, S85–S107
924 (1992).
925 32. Kryazhimskiy, S., Rice, D. P., Jerison, E. R. & Desai, M. M. Microbial evolution. Global epistasis
926 makes adaptation predictable despite sequence-level stochasticity. *Science* **344**, 1519–1522
927 (2014).
928 33. Butlin, R. K. Recombination and speciation. *Molecular Ecology* **14**, 2621–2635 (2005).
929 34. Kassen, R. The experimental evolution of specialists, generalists, and the maintenance of
930 diversity. *Journal of Evolutionary Biology* **15**, 173–190 (2002).
931 35. Levene, H. Genetic equilibrium when more than one ecological niche is available. *The American*
932 *Naturalist* **87**, 331–333 (1953).
933 36. Débarre, F. & Gandon, S. Evolution in heterogeneous environments: between soft and hard
934 selection. *The American Naturalist* **177**, E84–E97 (2011).
935 37. Nei, M. *Molecular Evolutionary Genetics*. (Columbia University Press, 1987).
936 38. Ratcliff, W. C., Denison, R. F., Borrello, M. & Travisano, M. Experimental evolution of
937 multicellularity. *Proceedings of the National Academy of Sciences* **109**, 1595–1600 (2012).
938 39. Burke, M. K., Liti, G. & Long, A. D. Standing genetic variation drives repeatable experimental
939 evolution in outcrossing populations of *Saccharomyces cerevisiae*. *Molecular Biology and*
940 *Evolution* **31**, 3228–3239 (2014).
941 40. Franssen, S. U., Kofler, R. & Schlötterer, C. Uncovering the genetic signature of quantitative trait
942 evolution with replicated time series data. *Heredity* **118**, 42–51 (2017).

943 41. Behe, M. J. Experimental evolution, loss-of-function mutations, and "the first rule of adaptive
944 evolution". *The Quarterly Review of Biology* **85**, 419–445 (2010).
945 42. Anderson, J. T., Lee, C.-R., Rushworth, C. A., Colautti, R. I. & Mitchell-Olds, T. Genetic trade-
946 offs and conditional neutrality contribute to local adaptation: Genetic basis of local adaptation.
947 *Molecular Ecology* **22**, 699–708 (2013).
948 43. Maclean, R. C. Adaptive radiation in microbial microcosms: Microbial diversification. *Journal of*
949 *Evolutionary Biology* **18**, 1376–1386 (2005).
950 44. Samani, P. & Bell, G. Experimental evolution of the grain of metabolic specialization in yeast.
951 *Ecology and Evolution* **6**, 3912–3922 (2016).
952 45. Savolainen, O., Lascoux, M. & Merilä, J. Ecological genomics of local adaptation. *Nature*
953 *Reviews Genetics* **14**, 807–820 (2013).
954 46. Barton, N. H. & Cara, M. A. R. D. The evolution of strong reproductive isolation. *Evolution* **63**,
955 1171–1190 (2009).
956 47. Flaxman, S. M., Wacholder, A. C., Feder, J. L. & Nosil, P. Theoretical models of the influence of
957 genomic architecture on the dynamics of speciation. *Molecular Ecology* **23**, 4074–4088
958 (2014).
959 48. Lowry, D. B., Rockwood, R. C. & Willis, J. H. Ecological reproductive isolation of coast and
960 inland races of *Mimulus guttatus*. *Evolution* **62**, 2196–2214 (2008).
961 49. Barton, N. & Bengtsson, B. O. The barrier to genetic exchange between hybridising populations.
962 *Heredity* **57**, 357 (1986).
963 50. Nicolaus, M. & Edelaar, P. Comparing the consequences of natural selection, adaptive phenotypic
964 plasticity, and matching habitat choice for phenotype–environment matching, population
965 genetic structure, and reproductive isolation in meta-populations. *Ecology and Evolution* **8**,
966 3815–3827 (2018).
967 51. Smith, J. M. Sympatric Speciation. *The American Naturalist* **100**, 637–650 (1966).
968 52. Filchak, K. E., Roethele, J. B. & Feder, J. L. Natural selection and sympatric divergence in the
969 apple maggot Rhagoletis pomonella. *Nature* **407**, 739–742 (2000).

970 53. Flaxman, S. M., Feder, J. L. & Nosil, P. Genetic Hitchhiking and the Dynamic Buildup of
971 Genomic Divergence During Speciation with Gene Flow. *Evolution* **67**, 2577–2591 (2013).
972 54. Sexton, J. P., Hangartner, S. B. & Hoffmann, A. A. Genetic Isolation by Environment or Distance:
973 Which Pattern of Gene Flow Is Most Common? *Evolution* **68**, 1–15 (2014).
974 55. Powell, T. H. Q. *et al.* Genetic Divergence Along the Speciation Continuum: The Transition from
975 Host Race to Species in Rhagoletis (diptera: Tephritidae). *Evolution* **67**, 2561–2576 (2013).
976 56. Roux, C. *et al.* Shedding Light on the Grey Zone of Speciation along a Continuum of Genomic
977 Divergence. *PLOS Biology* **14**, e2000234 (2016).
978 57. Wright, S. Evolution in Mendelian Populations. *Genetics* **16**, 97–159 (1931).
979 58. Mayr, E. *Change of genetic environment and evolution. In Evolution as a Process*. (Huxley JS,
980 Hardy AC, Ford EB, 1954).
981 59. Bulmer, M. G. Multiple Niche Polymorphism. *The American Naturalist* **106**, 254–257 (1972).
982 60. Fry, J. D. Multilocus Models of Sympatric Speciation: Bush Versus Rice Versus Felsenstein.
983 *Evolution* **57**, 1735–1746 (2003).
984 61. Nieuwenhuis, B. P. S. *et al.* Repeated evolution of self-compatibility for reproductive assurance.
985 *Nature Communications* **9**, 1639 (2018).
986 62. Curtsinger, J. W., Service, P. M. & Prout, T. Antagonistic Pleiotropy, Reversal of Dominance, and
987 Genetic Polymorphism. *The American Naturalist* **144**, 210–228 (1994).
988 63. Charlesworth, B. & Hughes, K. A. The maintenance of genetic variation in life history traits. in
989 *Evolutionary genetics: from molecules to morphology* vol. 1 369–391 (Cambridge Univ.
990 Press, Cambridge, U. K., 2000).
991 64. Phillips, P. C. Epistasis—the essential role of gene interactions in the structure and evolution of
992 genetic systems. *Nat Rev Genet* **9**, 855–867 (2008).
993 65. Carter, A. J. & Nguyen, A. Q. Antagonistic pleiotropy as a widespread mechanism for the
994 maintenance of polymorphic disease alleles. *BMC Medical Genetics* **12**, 160 (2011).
995 66. Hedrick, P. W., Ginevan, M. E. & Ewing, E. P. Genetic polymorphism in heterogeneous
996 environments. *Annual Review of Ecology and Systematics* **7**, 1–32 (1976).

997 67. Macnair, M. R. Why the evolution of resistance to anthropogenic toxins normally involves major
998 gene changes: the limits to natural selection. *Genetica* **84**, 213–219 (1991).
999 68. Ono, J., Gerstein, A. C. & Otto, S. P. Widespread genetic incompatibilities between first-step
1000 mutations during parallel adaptation of *Saccharomyces cerevisiae* to a common environment.
1001 *PLOS Biology* **15**, e1002591 (2017).
1002 69. Blount, Z. D., Lenski, R. E. & Losos, J. B. Contingency and determinism in evolution: Replaying
1003 life's tape. *Science* **362**, eaam5979 (2018).
1004 70. Jeffares, D. C. The natural diversity and ecology of fission yeast. *Yeast* **35**, 253–260 (2018).
1005 71. Heim, L. Construction of an h+S strain of *Schizosaccharomyces pombe*. *Current Genetics* **17**, 13–
1006 19 (1990).
1007 72. Forsburg, S. L. *Schizosaccharomyces pombe* strain maintenance and media. *Current Protocols in*
1008 *Molecular Biology* **64**, 13.15.1-13.15.5 (2003).
1009 73. Kassambara, A. & Mundt, F. Factoextra: extract and visualize the results of multivariate data.
1010 https://rdrr.io/cran/factoextra/ (2017).
1011 74. Martin, M. Cutadapt removes adapter sequences from high-throughput sequencing reads.
1012 *EMBnet.journal* **17**, 10 (2011).
1013 75. Bolger, A. M., Lohse, M. & Usadel, B. Trimmomatic: a flexible trimmer for Illumina sequence
1014 data. *Bioinformatics* **30**, 2114–2120 (2014).
1015 76. Wood, V. *et al.* The genome sequence of *Schizosaccharomyces pombe*. *Nature* **415**, 871 (2002).
1016 77. Li, H. & Durbin, R. Fast and accurate short read alignment with Burrows-Wheeler transform.
1017 *Bioinformatics* **25**, 1754–1760 (2009).
1018 78. McKenna, A. *et al.* The Genome Analysis Toolkit: A MapReduce framework for analyzing next-
1019 generation DNA sequencing data. *Genome Research* **20**, 1297–1303 (2010).
1020 79. Koboldt, D. C. *et al.* VarScan: variant detection in massively parallel sequencing of individual and
1021 pooled samples. *Bioinformatics* **25**, 2283–2285 (2009).
1022 80. Li, H. Toward better understanding of artefacts in variant calling from high-coverage samples.
1023 *Bioinformatics* **30**, 2843–2851 (2014).

1024 81. Cingolani, P. *et al.* A program for annotating and predicting the effects of single nucleotide
1025 polymorphisms, SnpEff: SNPs in the genome of *Drosophila melanogaster* strain w ^{1118} ; iso-2;
1026 iso-3. *Fly* **6**, 80–92 (2012).
1027 82. Lock, A. *et al.* PomBase 2018: user-driven reimplementation of the fission yeast database
1028 provides rapid and intuitive access to diverse, interconnected information. *Nucleic Acids Res*
1029 **47**, D821–D827 (2019).
1030 83. Nei, M. & Li, W. H. Mathematical model for studying genetic variation in terms of restriction
1031 endonucleases. *Proceedings of the National Academy of Sciences* **76**, 5269–5273 (1979).
1032 84. Weir, B. S. & Cockerham, C. C. Estimating F-statistics for the analysis of population structure.
1033 *Evolution* **38**, 1358 (1984).
1034 85. Haller, B. C. & Messer, P. W. SLIM 3: forward genetic simulations beyond the Wright–Fisher
1035 model. *Molecular Biology and Evolution* **36**, 632–637 (2019).
1036 86. Farlow, A. *et al.* The spontaneous mutation rate in the fission yeast *Schizosaccharomyces pombe*.
1037 *Genetics* **201**, 737–744 (2015).
1038 87. Munz, P., Wolf, K., Kohli, J. & Leupold, U. Genetics overview. *Molecular Biology of the Fission*
1039 *Yeast* 1–30 (1989).
1040 88. Tusso, S., Nieuwenhuis, B.P.S., Weissensteiner, B., Immler, S. & J.B.W., W. Experimental
1041 evolution of adaptive divergence under varying degrees of gene flow. (2020)
1042 doi:10.5281/ZENODO.4133489.
1043
1044
1045

Figure captions

Figure 1. Schematic illustration of the experiment.

a. Schematic of a 6-day experimental cycle including asexual population growth, ecological selection (top and bottom selection regime) and sexual reproduction (allopatry treatment shown as example). **b.** Representation of the four treatments differing in the amount of migration between fractions after ecological selection: i) allopatry: no gene flow, ii) parapatry: symmetric migration of 5% of cells (red and blue dashed lines), and full mixing (orange arrows) either iii) after sexual reproduction ('local mating') or iv) before sexual reproduction (sympatry). The number of populations per treatment for the α or β ancestral background is given at the bottom.

Figure 2. Fitness as a function of ecological selection and gene flow.

a. Fitness values of each population relative to the ancestral population for different fitness components (growth, sexual reproduction, performance after top or bottom selection) separated by ecological selection regime (top in blue and bottom in red; cf. **Figure 1b**), migration treatment (allopatric, parapatric, local mating, sympatric) and genetic background (α or β). Values > 1 provide evidence for adaptation. Each point represents the median value of 8 technical replicates per population. Note that for local mating and sympatry the entire population experiences top and bottom selection. Blue and red here refers to fitness values of the resulting top and bottom fractions (ecotypes) that experienced two additional cycles of selection in isolation. Statistical significance of Generalized Linear Model is indicated by asterisks (for statistical results see **Supplementary Table 1**; *$p < 0.05$, **$p < 0.01$, ***$p < 0.001$). Boxplots description: center line, median; box limits, upper and lower quartiles; whiskers, 1.5x interquartile range; points, outliers. **b.** Matrix of correlation coefficients of relative fitness values between fitness components per treatment and genetic background (Pearson's correlation across all 22 evolved populations (allopatry, parapatry) or subpopulations (local mating, sympatry); *$p<0.05$). The direction and strength of the relationship is indicated by colour (violet: negative; orange: positive) and the height of the bar, respectively.

1076

1077 **Figure 3. Partitioning of genetic variation and its relationship to fitness**

1078 **a**. Genetic variation and population structure relative to the ecological selection regime shown
1079 for the α genetic background. Each sub-plot shows the two main axes of variation across
1080 populations per treatment always including allopatric top and bottom as well as the ancestral
1081 population as reference (blue, red and black, respectively). PCA was performed on all genetic
1082 variants. For PCA across all populations combined for each ancestral background see
1083 **Extended Data Fig. 4**. **b.** Correlation between the two major PCA axes of genotypic
1084 variation (from **Figure 3a**) and variation in fitness (**Extended Data Fig. 2**) shown for
1085 allopatric α populations. Each dot represents one population.

1086

1087 **Figure 4. Candidate genetic variants under disruptive selection in α populations.**

1088 **a.** Example of a pair of variants with evidence for antagonistic pleiotropy. Each point shows
1089 the final allele frequency for the two loci in top or bottom populations from the allopatric
1090 treatment (frequencies for other treatments are shown in **Supplementary Figure 10**).
1091 Ancestral allele frequencies are shown in orange. Genetic variants are labelled with
1092 chromosome number, base position and alternative allele relative to the reference genome.
1093 The *grey area* indicates allele frequency combinations that would arise under a scenario of
1094 positive selection for both derived alleles; allele frequency combinations above the *diagonal*
1095 *line* provide unequivocal evidence for coupling of both derived mutations on a single
1096 haplotype. **b.** Predicted allele distribution for a pair of genetic variants under antagonistic
1097 pleiotropy. The derived allele for locus 1 (L1) is beneficial under environment 1 (top selection
1098 environment) but deleterious in environment 2 (bottom selection environment). The opposite
1099 occurs for locus 2 (L2). **c.** Representation of a fitness landscape where a population (orange
1100 circle) can adapt to the top or bottom environment (blue or red arrow, respectively) by
1101 increasing the frequency of the derived allele at locus 1 while decreasing the frequency for the
1102 derived allele at locus 2.

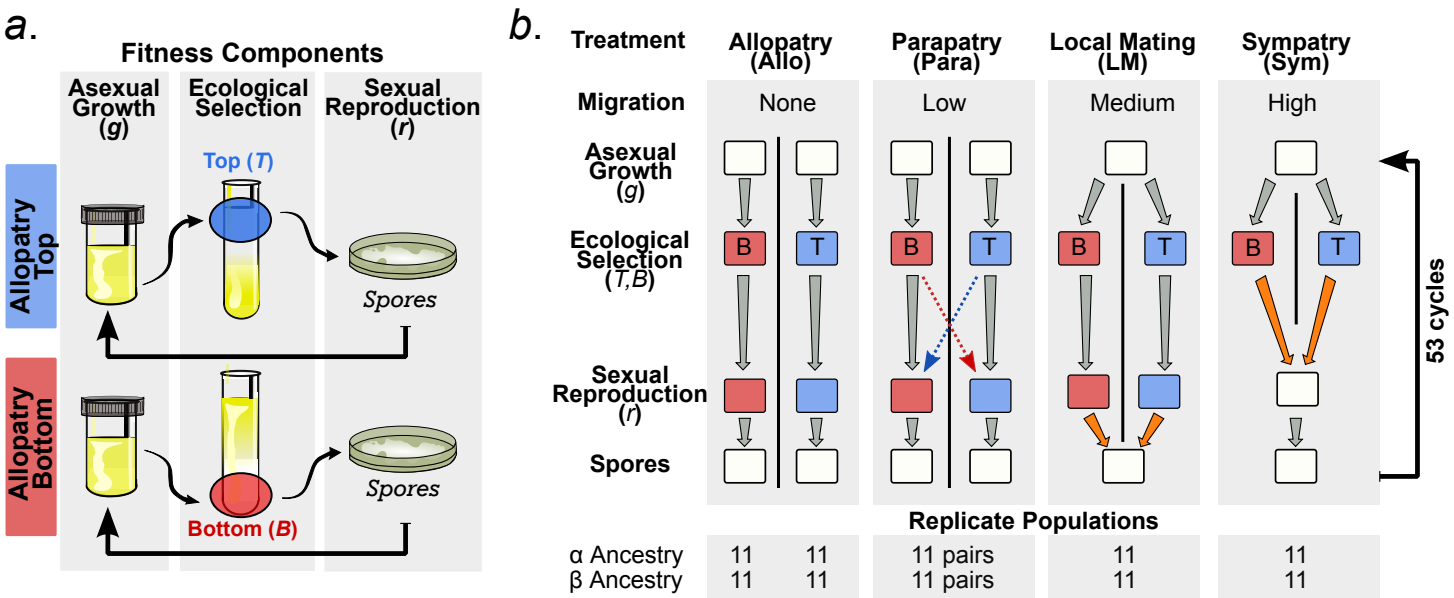
a.
Fitness Components
Asexual Growth (g)
Ecological Selection
Sexual Reproduction (r)
Allopatry Top
Allopatry Bottom
Top (T)
Bottom (B)
Spores
Spores
b.
Treatment
Allopatry (Allo)
Parapatry (Para)
Local Mating (LM)
Sympatry (Sym)
Migration
None
Low
Medium
High
Asexual Growth (g)
Ecological Selection (T,B)
Sexual Reproduction (r)
Spores
B
T
53 cycles
Replicate Populations
α Ancestry
β Ancestry
11 11
11 11
11 pairs
11 pairs
11
11
11
11

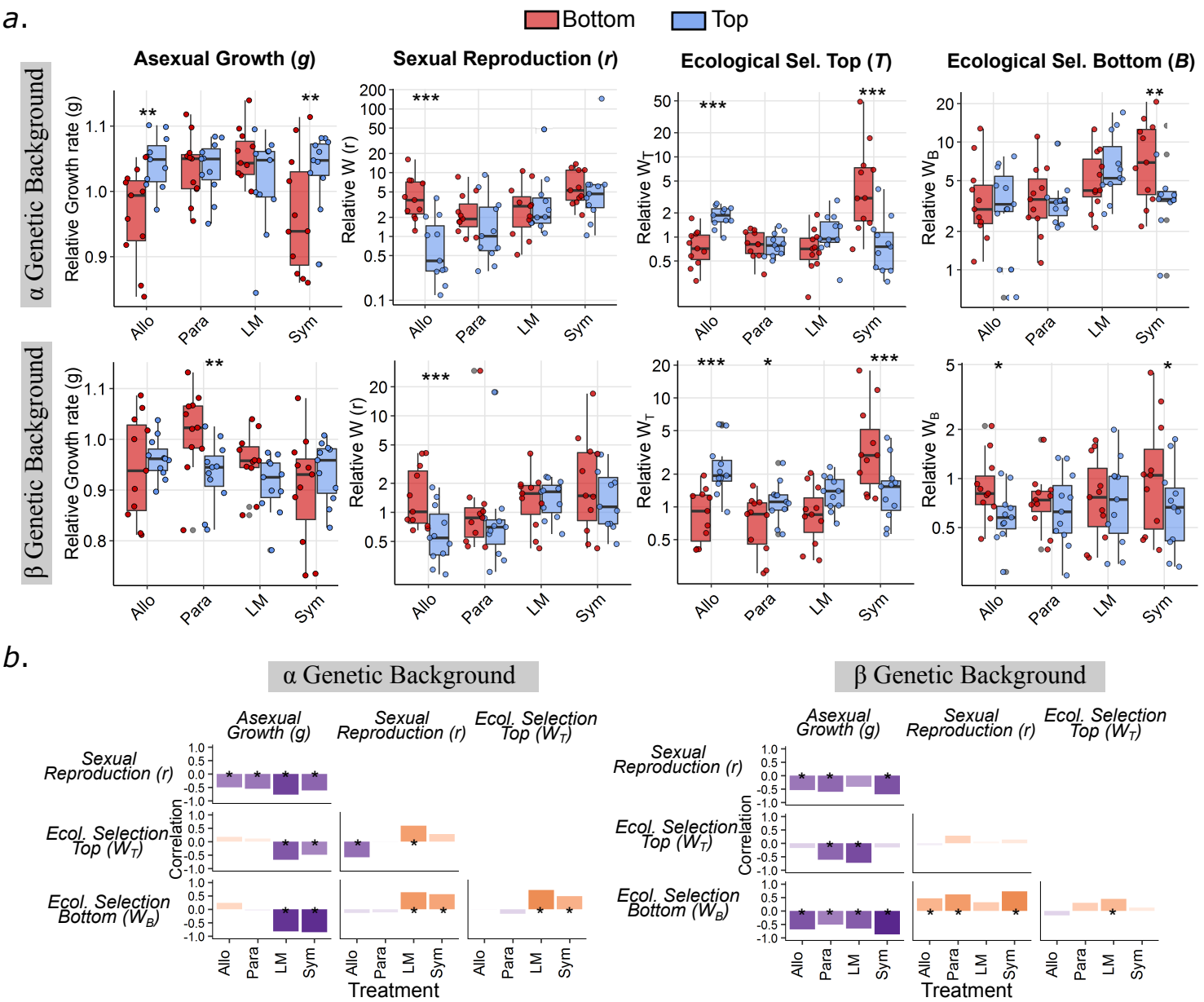
a.
Bottom
Top
Asexual Growth (g)
Sexual Reproduction (r)
Ecological Sel. Top (T)
Ecological Sel. Bottom (B)
α Genetic Background
β Genetic Background
Relative Growth rate (g)
Relative W (r)
Relative W_T
Relative W_B
Allo
Para
LM
Sym
b.
α Genetic Background
β Genetic Background
Asexual Growth (g)
Sexual Reproduction (r)
Ecol. Selection Top (W_T)
Ecol. Selection Bottom (W_B)
Correlation
Treatment

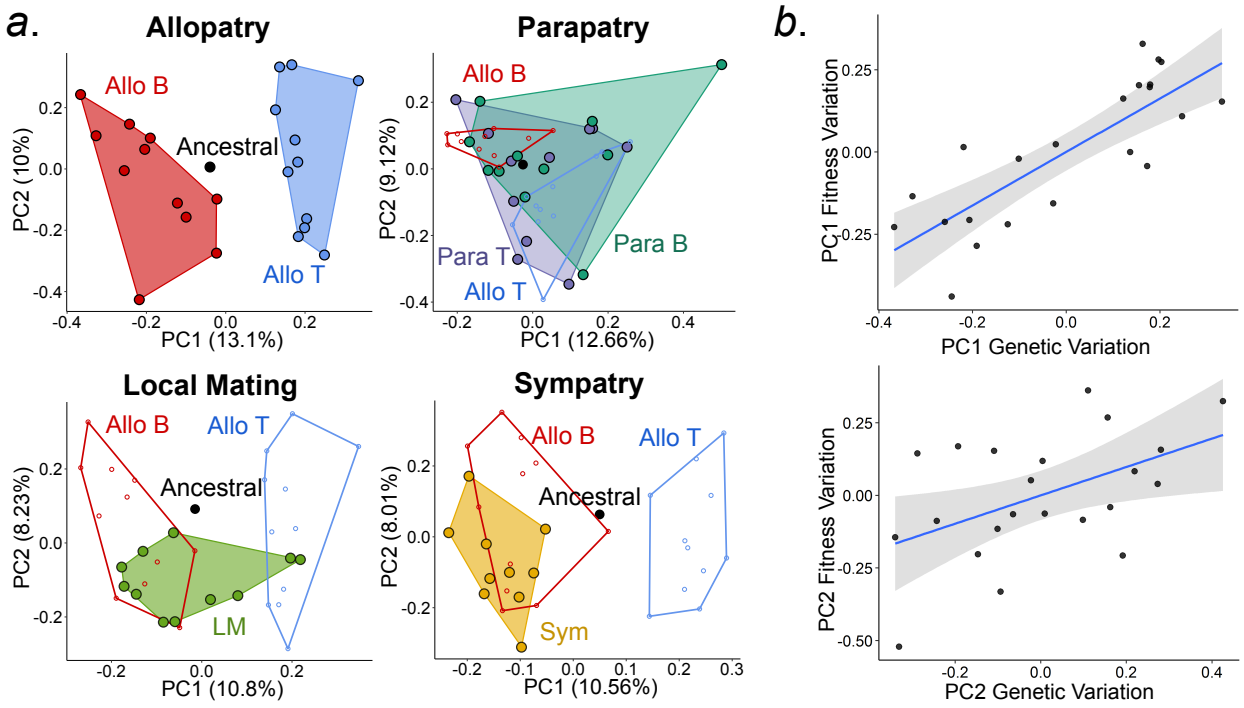
a.
Allopatry
Allo B
Ancestral
Allo T
PC2 (10%)
PC1 (13.1%)
Parapatry
Allo B
Para T
Allo T
Para B
PC2 (9.12%)
PC1 (12.66%)
Local Mating
Allo B
Allo T
Ancestral
LM
PC2 (8.23%)
PC1 (10.8%)
Sympatry
Allo B
Allo T
Ancestral
Sym
PC2 (8.01%)
PC1 (10.56%)
b.
PC1 Fitness Variation
PC1 Genetic Variation
PC2 Fitness Variation
PC2 Genetic Variation

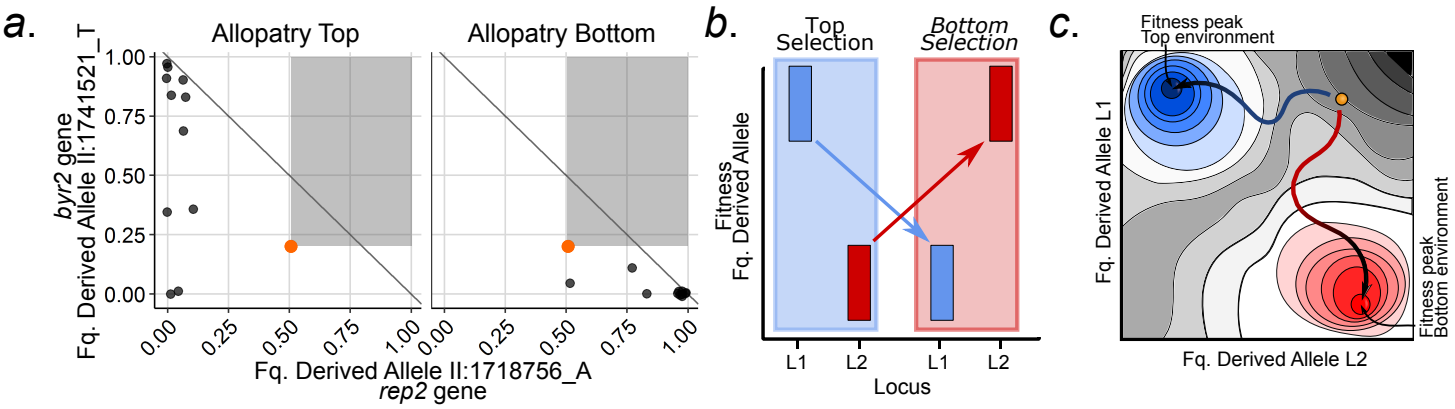
a.
Allopatry Top
Allopatry Bottom
byr2 gene
Fq. Derived Allele II:1741521_T
1.00
0.75
0.50
0.25
0.00
0.00
0.25
0.50
0.75
1.00
Fq. Derived Allele II:1718756_A
rep2 gene
b.
Top Selection
Bottom Selection
Fitness
Fq. Derived Allele
L1
L2
L1
L2
Locus
c.
Fitness peak
Top environment
Fq. Derived Allele L1
Fq. Derived Allele L2
Fitness peak
Bottom environment